SPANDIDOS PUBLICATIONS

ONCOLOGY REPORTS 25: 1473-1480, 2011

Paclitaxel-induced apoptosis is blocked by camptothecin in human breast and pancreatic cancer cells

DUANE P. JEANSONNE[1], GAR YEE KOH[1], FANG ZHANG[1], HEATHER KIRK-BALLARD[2], LAURA WOLFF[1], DONG LIU[1], KENNETH EILERTSEN[2] and ZHIJUN LIU[1]

[1]School of Renewable Natural Resources, Louisiana State University Agricultural Center, Baton Rouge, LA 70803; [2]Pennington Biomedical Research Center, Louisiana State University, Baton Rouge, LA 70808, USA

Received November 16, 2010; Accepted January 11, 2011

DOI: 10.3892/or.2011.1187

Abstract. The combination of paclitaxel (PTX) and topoisomerase I inhibitors such as camptothecin (CPT) constitutes a therapeutic strategy based on anticipated synergism. However, previous *in vitro* studies have generated contradictory findings for this strategy. The interaction between these drugs can be synergistic or antagonistic, depending on the cell type examined. To gain additional insight into this promising yet controversial strategy, we investigated the interaction between PTX and CPT in three different cell lines (PANC-1, MDA-MB-231 and HL-60) and explored possible underlying mechanisms of synergy or antagonism. Using a novel solubilizing natural compound, rubusoside, water-insoluble PTX and CPT were solubilized to enable the comparison of the effects of single drugs and their combination on cell viability. Intracellular drug concentrations were quantified to examine the effect of CPT on cellular uptake and accumulation of PTX. Flow cytometry and quantitative real-time PCR gene array analyses were used to explore the mechanisms behind the interaction between PTX and CPT. Our studies confirmed that rubusoside-solubilized PTX or CPT maintained cytotoxicity, causing significant reductions in cell viability. However, the efficacy of the combination of PTX and CPT produced varied results based on the cell line tested. CPT antagonistically reduced the cytotoxic activity of PTX in PANC-1 and MDA-MB-231 cells. The effect of CPT on the cytotoxicity of PTX was less pronounced in HL-60 cells, showing neither synergy nor antagonism. Analysis of apoptosis by flow cytometry revealed that upon co-treatment with CPT, apoptosis induced by PTX was attenuated in PANC-1 and MDA-MB-231 cells. In agreement with our cytotoxicity findings, no synergistic or antagonistic effects on apoptosis were observed in HL-60 cells. The antagonism in PANC-1 and MDA-MB-231 cells was not a result of reduced PTX uptake and accumulation because the amount of intracellular PTX was not altered upon co-treatment with CPT. Moreover, higher expression of anti-apoptosis-related transcripts (*BCL2L10*, *CFLAR*, *HIP1* and *TRADD*) in PANC-1 cells was observed upon combination treatment over PTX treatment alone. Although exact underlying mechanisms are unknown, the suspected CPT-dependent reduction of intracellular PTX accumulation was ruled out. The findings of antagonism and increased anti-apoptotic gene transcription serve as a precaution to the design of combination drug strategies where a synergistic interaction may not exist.

Introduction

The potent chemotherapeutic agent paclitaxel (PTX) belongs to the chemical class known as the taxanes, which are produced by the Pacific Yew (*Taxus brevifolia*) and other *Taxus* species (1). PTX acts by blocking cell mitosis through the stabilization of microtubules, leading to cell cycle arrest preferentially in the G_2/M phase and apoptosis (2-4). Currently, PTX is used to treat multiple cancer types, including ovarian, breast, head and neck, and lung tumors (5). PTX has shown varied clinical efficacy in combination with several cancer therapeutics such as trastuzumab (Herceptin®), carboplatin, cisplatin, 5-fluorouracil, gemcitabine and topoisomerase I (topo I) inhibitors (1,6-8).

Camptothecin (CPT) is a quinoline alkaloid produced by the tree *Camptotheca acuminata* in the family of *Nyssaceae*. Due to the poor water solubility, several analogs of CPT have been developed over the years (9). Two such analogs, topotecan (Hycamtin®) and irinotecan (Camptosar®), are currently approved drugs in the US for the treatment of ovarian, small-cell lung and colorectal cancers (10-12). Studies have shown that these potent cytotoxic agents inhibit DNA topo I resulting in the blockade of the DNA religation step after strand cleavage and concomitant apoptosis of the target cell (13,14).

Combination therapy is a common approach for the treatment of most cancer types and often results in survival advantage over monotherapy. Based on their distinct mechanisms of action, PTX and CPT may represent a promising

Correspondence to: Dr Zhijun Liu, School of Renewable Natural Resources, Louisiana State University Agricultural Center, 143 H.D. Wilson Building, Baton Rouge, LA 70803, USA
E-mail: zhiliu@lsu.edu

Key words: paclitaxel, camptothecin, cancer, synergism, antagonism, apoptosis

combination strategy. Targeting two different cellular proteins simultaneously by a combination of two compounds should, in theory, lead to increased cell death. In fact, clinical trials have been conducted to assess the efficacy of PTX and topo I inhibitors as a combination therapy against cancer (8,15,16). However, pre-clinical *in vitro* efficacy studies on the PTX and topo I inhibitor combination have yielded conflicting results. An analysis of Taxol® (PTX) in combination with topotecan against teratocarcinoma cell lines revealed a synergistic interaction between these two drugs (17), whereas an antagonistic interaction between PTX and topotecan was demonstrated in A549 lung cancer cells (18). In another study, the combination of Taxol® (PTX) and topotecan was examined against several tumors of different histological origin and found to be synergistic or antagonistic, depending on the cell type (19). These contradictory findings have raised doubts on the utility of a combination strategy that is based solely on predicted synergy. Consequently, this strategy must be re-examined to clarify the conflicting reports and broaden our limited knowledge on the mechanisms of interaction between PTX and CPT. This re-examination effort was enabled because of the critical discovery of the solubilizing properties of rubusoside, which are applicable to PTX and CPT alone or in combination. Therefore, the purposes of this study were to confirm the biological applicability of this novel approach for solubilizing PTX and CPT, to determine their nature of interaction in different cell lines with regard to cytotoxicity, and to explore the underlying mechanisms of action behind the observed cellular phenotypes from the aspects of cellular uptake and apoptosis-related gene expression.

Materials and methods

Reagents. PTX with purity of 99% was purchased from LKT Laboratories, Inc. (St. Paul, MN). CPT and HPLC grade formic acid were purchased from Sigma Chemical Co. (St. Louis, MO). Acetonitrile, methanol and water were of HPLC grade and purchased from Mallinckrodt Baker Inc. (Phillipsburg, NJ). DMSO was purchased from Fisher Scientific (Fair Lawn, NJ). Rubusoside, a non-toxic solubilizing agent, was isolated from the plant *Rubus suavissimus* S. Lee (Rosaceae) by our laboratory and structurally elucidated by NMR and MS analyses. The purity was determined to be >98% by HPLC-UV analysis.

Drug solubilization. To solubilize PTX, rubusoside (10 g) was weighed and dissolved in 100 ml of distilled and deionized water by sonication for 60 min at 60˚C. PTX (25.0 mg) was added to the rubusoside water solution, which was sonicated for 60 min at 60˚C, then autoclaved for 60 min. The solution was then passed through a 0.45-μm filter. An additional amount of PTX (30.0 mg) was then added to the filtered solution and sonicated for 30 min. The solution was autoclaved for 60 min, passed through a 0.45 μm filter and stored at 37˚C. To solubilize CPT, rubusoside (2 g) was weighed and dissolved in 20 ml of distilled and deionized water by sonication for 60 min at 60˚C. CPT (10 mg) was added to the rubusoside water solution, which was sonicated for 60 min at 60˚C, then autoclaved for 30 min. The solution was passed through a 0.45-μm filter and stored at 37˚C.

Stability of PTX. To determine the stability of PTX in solution and with CPT, a set of rubusoside-solubilized PTX solutions containing 1-10 μg/ml PTX was mixed with rubusoside-solubilized CPT water solutions containing 2 μg/ml CPT. All water solutions, which contained 10% w/v rubusoside, were diluted 100-fold in water to a final rubusoside concentration of 0.1%. In previous studies, DMSO concentrations as low as 0.1% have been used to solubilize paclitaxel (20). Therefore, a parallel set of PTX solutions (1-10 μg/ml) in 2 μg/ml CPT solubilized by 100% DMSO were prepared and then were each diluted 100-fold with water to a final DMSO concentration of 1% v/v. These DMSO-solubilized solutions contained identical drug concentrations based on mathematical calculations of the dilution factors and were meant to be used as controls for the rubusoside-solubilized drug solutions. Drug solutions were stored at 25˚C for 3 days before detection by HPLC-MS.

HPLC protocol for drug preparations. HPLC was used to analyze PTX and CPT in the solubilized solutions. The system included a pump, an on-line degasser, a column heater compartment, an auto-sampler, and a photodiode array (PDA) detector (Waters, Milford, MA). Empower^{1} workstation software was used for the control of the equipment, acquisition and processing of data. All of the analyses were performed on a reversed-phase Prevail ODS HPLC column (150x2.1 mm i.d.; 3 μm). Analysis of PTX was performed at 30˚C with a mobile phase of 0.25% formic acid water solution, acetonitrile and methanol (40/40/20, v/v/v) at 0.4 ml/min. The injection volume of sample was 1 μl. The PDA detection range was set to wavelengths of 200-600 nm and chromatograms were developed at 230 nm for PTX and 205 nm for rubusoside. Analysis of CPT was performed at 30˚C with a mobile phase of 0.02% formic acid water solution and acetonitrile (68/32, v/v) at 0.4 ml/min. The injection volume of sample was 3 μl. The PDA detector was set to wavelengths of 200-600 nm and chromatograms were developed at 368 nm for CPT and 205 nm for rubusoside.

HPLC-MS protocol for stability experiments. HPLC-MS was used to analyze PTX stability. The system included a pump, an on-line degasser, a column heater compartment, an auto-sampler, a photodiode array (PDA) detector and an EMD1000 mass spectrometer with an ESI interface and a TOF mass analyzer (Waters, Milford, MA). Empower^{1} workstation software was used for the control of the equipment, acquisition and processing of data. All of the analyses were performed on a reversed-phase Prevail ODS HPLC column (150x2.1 mm i.d.; 3 μm) at 30˚C with a mobile phase of 0.02% formic acid water solution, acetonitrile and methanol (37/42/21, v/v/v) at 0.35 ml/min. The injection volume of sample was 20 μl. The elution from HPLC was introduced into a mass spectrometer with an ESI interface and the data were collected with the following settings: a positive scan, 3.5 kV capillary, 25.00 V cone, 1.00 V extractor, 120˚C source temperature, 400˚C desolvation temperature, 50 l/Hr cone gas flow (N_2) and 400 l/Hr desolvation gas flow (N_2). The selected ion recording (SIR) scan mode at m/z 876.4 $[M_{PTX}+Na]^+$ was set for PTX detection.

HPLC-MS protocol for intracellular PTX accumulation experiments. Cell samples were freeze-dried and resuspended

with 2.0 ml of tert-butyl methyl ether. Following sonication for 60 min, samples were centrifuged at 20800 rcf for 10 min. The upper, organic layer (15 ml) was quantitatively transferred to a 2-ml tube and dried under a gentle stream of nitrogen gas at 25˚C. The sample was reconstituted in 300 μl of methanol and the solution was vortexed. After centrifugation at 20800 rcf for 10 min, 5 μl of the solution was injected into the HPLC-MS system. Analyses were performed on a reversed-phase Prevail ODS HPLC column (150x2.1 mm i.d.; 3 μm) at 30˚C with a mobile phase of 0.02% formic acid water solution and methanol (32/68, v/v) at 0.25 ml/min. The elution from HPLC was introduced into a mass spectrometer with an ESI interface. Analysis was carried out as described for the PTX stability experiments.

Cell lines and culture conditions. The human pancreatic carcinoma (PANC-1), breast carcinoma (MDA-MB-231) and leukemia (HL-60) cell lines were obtained from the American Type Culture Collection (ATCC) and were maintained at 37˚C in a humidified atmosphere with 5% CO_2. PANC-1 and MDA-MB-231 cells were cultured in Dulbecco's modified Eagle's medium (DMEM) supplemented with 10% fetal bovine serum, HEPES, penicillin-streptomycin, sodium pyruvate, L-glutamine and non-essential amino acids. HL-60 cells were cultured in Iscove's modified Dulbecco's medium (IMDM) supplemented with 20% fetal bovine serum, insulin-transferrin-selenium, penicillin-streptomycin, sodium pyruvate, L-glutamine and non-essential amino acids. All cell culture materials were purchased from Invitrogen Corp. (Carlsbad, CA).

Cell viability assay. To evaluate the cytotoxicity of PTX and CPT, *in vitro* cell viability assays were conducted using the 3-(4,5-dimethylthiazol-2-yl)-5-(3-carboxymethoxyphenyl)-2-(4-sulfophenyl)-2H-tetrazolium (MTS) assay (Promega, Madison, WI). PANC-1 and MDA-MB-231 cells were added to 96-well plates at $1x10^4$ cells/well and allowed to adhere overnight. HL-60 cells were plated at $7.5x10^4$ cells/well and incubated overnight. The cells were then treated with various drug concentrations ranging from 0.2 to 100 ng/ml in medium. The plate was incubated at 37˚C for 3 days followed by addition of fresh drug-containing medium and incubation for another 3 days. On day six, a 20-μl aliquot of MTS solution premixed with phenazine methosulfate was added directly to each well and the plate was incubated at 37˚C for another 120 min. Absorbance was measured at a wavelength of 490 nm using a Bio-Rad Microplate Reader (Hercules, CA). Percent viability was calculated as cell viability relative to vehicle (rubusoside)-treated control (100%).

Flow cytometry. Apoptosis of treated cells was evaluated using the Vybrant® Apoptosis Assay Kit no. 2 from Molecular Probes (Eugene, OR). PANC-1 and MDA-MB-231 cells were plated at $1x10^5$ cells/well in 12-well plates and allowed to adhere overnight. HL-60 cells were plated at $2.5x10^5$ cells/well and incubated overnight. Cells were treated with PTX or a combination of PTX and CPT for 3 days followed by addition of fresh drug-containing medium and incubation for another 3 days. After treatment, adherent cells were harvested by trypsinization. All cell lines were washed 1X with PBS and resuspended in Annexin V-binding buffer containing Alexa Fluor 488 Annexin V and propidium iodide (PI) diluted according to manufacturer's protocol. Cells were incubated for 15 min at 25˚C in the dark followed by analysis using a BD FACSCalibur flow cytometer (BD Biosciences, San Jose, CA).

Intracellular PTX accumulation experiments. PANC-1 and MDA-MB-231 cells were plated at $1x10^5$ cells/well in 12-well plates and allowed to adhere overnight. HL-60 cells were plated at $2.5x10^5$ cells/well and incubated overnight. Cells were treated (n=3) with PTX or a combination of PTX and CPT for 3 days followed by addition of fresh drug-containing medium and incubation for another 3 days. After treatment, cells were washed with PBS and lysed with 0.5% SDS. A similar approach using SDS lysis has been reported in previous studies (21). Lysate samples were assayed for protein content by the bicinchoninic acid (BCA) protein assay (Pierce, Rockford, IL). The remainder of each sample was frozen at -80˚C and subjected to freeze-drying (FreeZone 4.5, Labconco, Kansas City, MO). Samples were resuspended and analyzed for PTX using the HPLC methods described above. Cellular uptake was calculated as a ratio of PTX detected (ng) per amount of cellular protein (mg).

TaqMan human apoptosis array. PANC-1 cells were plated at $1x10^5$ cells/well in 12-well plates and allowed to adhere overnight. Cells were treated with PTX or a combination of PTX and CPT for 3 days followed by addition of fresh drug-containing medium and incubation for another 3 days. After treatment, cells were harvested and mRNA was obtained using the RNeasy Mini Kit (Qiagen, Carlsbad, CA). mRNA was reverse transcribed to cDNA using the high capacity cDNA reverse transcription kit (Applied Biosystems, Carlsbad, CA). Quantitative real-time PCR was then performed by using the TaqMan® Human Apoptosis Array (Applied Biosystems) to examine the relative expression levels of 93 known human target genes, in addition to 3 endogenous controls (18S, ACTB, GAPDH). The 93 genes are categorized in multiple target classes or pathways associated with apoptosis of the cell. A relative increase or decrease in gene expression of particular genes was observed in the treatment groups as compared to controls.

Statistical analysis. Cell viability and apoptosis data were analyzed using the Statistical Analysis System software (SAS, Cary, NC). Statistical differences in cell viability and apoptosis between treatment groups were determined by one-way analysis of variance (ANOVA). Tukey's post-hoc test was performed to compare group differences. Statistical analyses for the TLDA array were performed by a two sample equal variance, one-tailed t-test. All data are expressed as the means ± SEM and P-values ≤0.05 were considered significant.

Results

Stability of rubusoside-solubilized PTX. Rubusoside-solubilized PTX solutions containing 1-10 μg/ml PTX in 2 μg/ml CPT (10% w/v rubusoside) were stable in solution and after dilution by 100 fold (0.1% w/v rubusoside). A

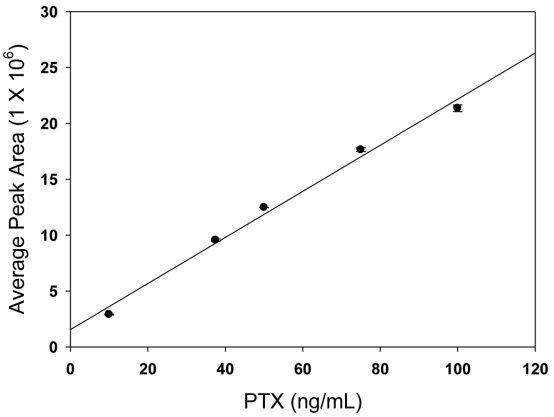

Figure 1. Overlay plot of actual PTX concentrations (solid circles) against calculated PTX concentrations (line). PTX was solubilized in 10% w/v rubusoside and this sample was serially diluted 100-fold. Diluted samples were analyzed by HPLC-MS. Each data point represents the means ± SEM (n=2).

plot of calculated PTX concentrations after dilution versus actual PTX detected by HPLC-MS (peak area) was fit to the equation of a line with an R^2 value of 0.99 (Fig. 1). However, DMSO-solubilized PTX, in solution with 2 μg/ml CPT, was not detectable by HPLC-MS after being diluted to a final concentration of 1% v/v DMSO (data not shown).

Cytotoxicity of PTX or CPT alone. The cytotoxicity of rubusoside-solubilized PTX and rubusoside-solubilized CPT was assessed against PANC-1, MDA-MB-231 and HL-60 cell lines. DMSO-solubilized PTX was not used as controls in any of the cytotoxicity evaluations because PTX was not detectable in such preparations. PTX and CPT each reduced the viability of all cell lines in a dose-dependent manner with rubusoside alone (vehicle) showing no cytotoxic effects (Fig. 2). PTX exhibited potent effects on cell viability with IC_{50} values of 12.5 ng/ml (14.6 nM) and 4.3 ng/ml (5.0 nM) against PANC-1 and MDA-MB-231 cells, respectively (Fig. 2). However, PTX had the most potent activity against HL-60 cells (IC_{50}=2.6 ng/ml or 3.0 nM; Fig. 2). CPT was less effective at reducing cell viability of PANC-1 (IC_{50}=37.5 ng/ml or 107.6 nM) and MDA-MB-231 (IC_{50}=47.8 ng/ml or 137.2 nM) cells as compared to PTX (Fig. 2). However, CPT was as effective as PTX at reducing HL-60 cell viability (IC_{50}=2.9±0.2 ng/ml or 8.3 nM; Fig. 2).

Effect of PTX and CPT combination treatment on cell viability. To determine whether PTX and CPT interact synergistically, combination studies were performed. Interestingly, when PANC-1 cells were exposed to PTX and CPT in combination, an overlay of data from Fig. 2 shows that cell viability was increased, not decreased, over PTX treatment alone (Fig. 3). When treated with PTX alone, PANC-1 cell viability decreased in a dose-dependent manner to 28.7% at 100 ng/ml PTX. In contrast, the addition of 6 ng/ml CPT to the 100 ng/ml PTX solution resulted in a reduction in cytotoxicity and a PANC-1 cell viability of 46.1% after treatment. Furthermore, it appears that the addition of CPT to the PTX solutions blocked the effect of PTX on the cancer cells completely, erasing the dose response pattern observed in these cells treated with PTX alone (Fig. 3). This antagonism of PTX by CPT was even more pronounced in MDA-MB-231 cells. When exposed to 20 ng/ml CPT in the presence of increasing PTX concentrations, MDA-MB-231 cell viability was not reduced to the extent of cells treated with PTX alone (Fig. 3). Also in agreement with the antagonistic interaction observed in PANC-1 cells, the addition of CPT appeared to completely abolish the cytotoxic contribution of PTX against MDA-MB-231 cells. Interestingly, in HL-60 cells this antagonism between PTX and CPT was not detected (Fig. 3).

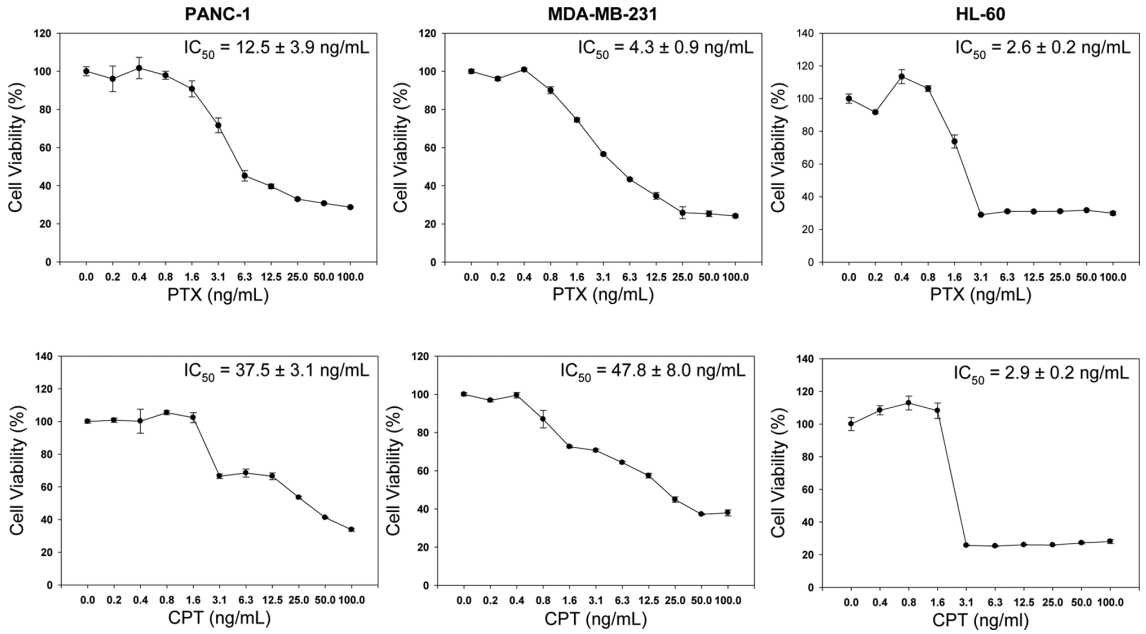

Figure 2. Cell viability (% of vehicle control) of three human cancer cell lines treated with rubusoside-solubilized PTX (upper) or rubusoside-solubilized CPT (lower). Each data point represents the means of 5 wells. Each experiment was repeated at least twice. Vertical bars represent standard error of the means. IC_{50}, drug concentration required for 50% inhibition of cell viability.

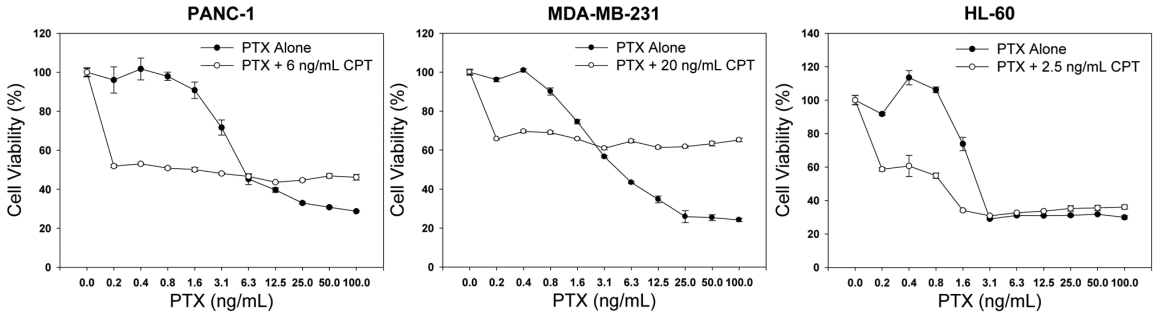

Figure 3. Cell viability (% of vehicle control) of PANC-1, MDA-MB-231 and HL-60 cells treated with PTX alone or PTX and CPT combination. Each data point represents the means of 5 wells. Vertical bars represent standard error of the means.

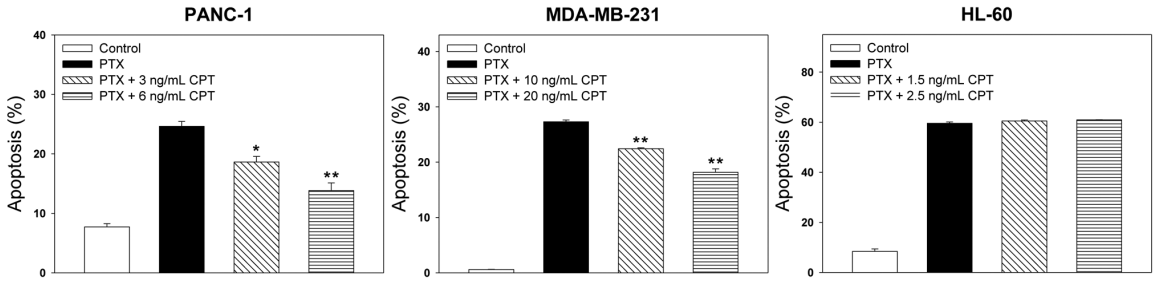

Figure 4. Effects of CPT on apoptosis induced by PTX in PANC-1, MDA-MB-231 and HL-60 cells. Apoptotic cells were stained with Annexin V and analyzed by fluorescence activated cell sorting. Plots show the percentages of Annexin-positive cells after drug treatments. The data represent the means ± SEM (n=3). A P-value ≤0.05 (*) or ≤0.01 (**) indicates a significant change relative to treatment with PTX alone.

The viability of the HL-60 cells continued to decrease with increasing PTX concentrations with or without the presence of 1.5 or 2.5 ng/ml CPT (data not shown).

Effect of PTX and CPT combination treatment on apoptosis. To gain insight into the mechanism of interaction between PTX and CPT, flow cytometry was used to evaluate the effect of single and combination drug treatments on tumor cell apoptosis. Treatment of all three cell lines with PTX alone induced an increase in apoptosis, as determined by Annexin V staining (Fig. 4). However, when PANC-1 and MDA-MB-231 cells were treated with the PTX and CPT combination, a significant reduction in apoptosis was observed compared to cells treated with PTX alone. Furthermore, this antagonistic effect was dose-dependent with respect to CPT, whereby increasing CPT concentrations resulted in a stronger antagonism of apoptosis (Fig. 4). In contrast, combination treatment of HL-60 cells did not change the pattern of PTX-induced apoptosis, as the amount of apoptosis was relatively equal in all treatment groups (Fig. 4). This result is in agreement with the cell viability data shown in Fig. 3.

Intracellular accumulation of PTX after combination treatment with CPT. A possible mechanism by which the apoptotic effects of PTX were attenuated upon co-treatment with CPT is through a decrease in cellular uptake or an increase in efflux of PTX from the cell. In either case, this would result in less PTX accumulation in the cells for the duration of the treatments. Therefore, an intracellular drug accumulation analysis was conducted, where the intracellular concentrations of PTX were assessed in PANC-1, MDA-MB-231 and HL-60 cells treated with PTX alone or in combination with CPT (Fig. 5). Co-treatment of cells with 6 ng/ml CPT (PANC-1) or 20 ng/ml CPT (MDA-MB-231) did not result in a decrease of intracellular PTX concentrations. Furthermore, treatment of PANC-1 cells with the combination resulted in a statistically significant increase in intracellular concentrations of PTX (Fig. 5), even though the cell viability increased and apoptosis decreased

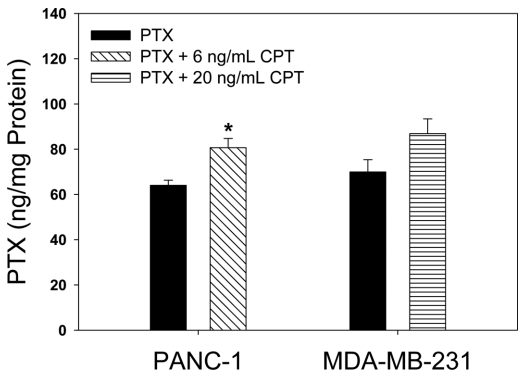

Figure 5. Accumulation of PTX in PANC-1 or MDA-MB-231 cancer cells treated with 100 ng/ml PTX alone or PTX with either 6 ng/ml CPT in PANC-1 or 20 ng/ml CPT in MDA-MB-231 for 6 days. The data represent the means ± SEM (n=3). A P-value ≤0.05 (*) indicates a significant change relative to treatment with PTX alone.

Table I. Fold change in expression of apoptotic-related genes in PANC-1 cells treated with PTX and CPT in combination compared to treatment with PTX alone.

Gene	ID	Fold change: 100 ng/ml PTX + 2 ng/ml CPT	Fold change: 100 ng/ml PTX + 4 ng/ml CPT
18S	Hs99999901_s1	Endo	Endo
ACTB	Hs99999903_m1	Endo	Endo
APAF1	Hs00559441_m1	2.04 ↑[b]	2.66 ↑[b]
BAD	Hs00188930_m1	NC	1.72 ↑
BAK1	Hs00832876_g1	1.67 ↓[a]	1.11 ↓
BAD	Hs00751844_s1	1.67 ↑	2.14 ↑
BBC3	Hs00248075_m1	NC	NC
BCAP31	Hs01036137_m1	1.61 ↑	1.69 ↑
BCL10	Hs00961847_m1	NC	NC
BCL2A1	Hs00187845_m1	1.96 ↑	NC
BCL2	Hs00608023_m1	NC	1.55 ↑
BCL2L10	Hs00368095_m1	1.53 ↑	2.25 ↑[b]
BCL2L11	Hs00708019_s1	1.52 ↑	2.30 ↑[a]
BCL2L13	Hs00209789_m1	1.81 ↑	2.41 ↑[a]
BCL2L14	Hs00373302_m1	ND	ND
BCL2L1	Hs00169141_m1	1.74 ↑	1.98 ↑
BCL2L2	Hs00187848_m1	1.41 ↑	1.62 ↑
BCL3	Hs00180403_m1	NC	NC
BID	Hs00609632_m1	1.33 ↑	1.41 ↑
BIK	Hs00154189_m1	3.51 ↑[a]	5.32 ↑[b]
BIRC1	Hs01847653_s1	2.18 ↓[a]	2.09 ↓[a]
BIRC2	Hs00236911_m1	NC	NC
BIRC3	Hs00985031_g1	NC	NC
BIRC4	Hs00745222_s1	2.61 ↓	1.70 ↓
BIRC5	Hs00977611_g1	1.88 ↑	1.80 ↑[a]
BIRC6	Hs00212288_m1	2.04 ↑[b]	2.42 ↑[b]
BIRC7	Hs00223384_m1	1.63 ↑	1.97 ↑
BIRC8	Hs01057786_s1	ND	ND
BNIP3	Hs00969291_m1	1.72 ↑	1.74 ↑
BNIP3L	Hs00188949_m1	1.69 ↑	2.41 ↑[a]
BOK	Hs00261296_m1	1.88 ↑	2.52 ↑[a]
CARD15	Hs00223394_m1	4.38 ↑	3.86 ↑
CARD4	Hs00196075_m1	1.75 ↑	2.42 ↑[a]
CARD6	Hs00261581_m1	ND	ND
CARD9	Hs00364485_m1	NC	1.47 ↑
CASP10	Hs01017902_m1	2.80 ↑[a]	4.24 ↑[b]
CASP14	Hs00201637_m1	ND	ND
CASP1	Hs00354836_m1	3.97 ↑[c]	5.86 ↑[b]
CASP2	Hs00892481_m1	2.58 ↑[b]	3.64 ↑[b]
CASP3	Hs00263337_m1	1.51 ↑	2.28 ↑[a]
CASP4	Hs01031947_m1	1.91 ↑[b]	2.14 ↑[a]
CASP5	Hs00362072_m1	ND	ND
CASP6	Hs00154250_m1	2.21 ↑[a]	2.56 ↑[a]
CASP7	Hs00169152_m1	2.17 ↑[a]	2.72 ↑[a]
CASP8AP2	Hs01594281_m1	1.80 ↑[a]	1.78 ↑[a]
CASP8	Hs01018151_m1	1.77 ↑	2.07 ↑[a]
CASP9	Hs00154260_m1	ND	ND
CFLAR	Hs00153439_m1	2.13 ↑[a]	2.49 ↑[a]
CHUK	Hs00989502_m1	NC	1.67 ↑
CRADD	Hs01011159_g1	1.56 ↑	1.91 ↑
DAPK1	Hs00234480_m1	1.61 ↑	1.79 ↑
DEDD2	Hs00370206_m1	1.05 ↑	1.35 ↑
DEDD	Hs00172768_m1	1.48 ↑	1.96 ↑
DIABLO	Hs00219876_m1	1.40 ↑	2.21 ↑[a]
ESRRBL1	Hs00215973_m1	1.27 ↑	1.69 ↑
FADD	Hs00538709_m1	1.53 ↑[a]	1.81 ↑[a]
FAS	Hs00236330_m1	2.71 ↑	5.21 ↑
FASLG	Hs00181225_m1	ND	ND
GAPDH	Hs99999905_m1	Endo	Endo
HIP1	Hs00193477_m1	2.27 ↑[a]	2.93 ↑[a]
HRK	Hs00705213_s1	ND	ND
HTRA2	Hs00376860_g1	1.26 ↑	1.56 ↑
ICEBERG	Hs01043258_m1	NC	NC
IKBKB	Hs00395088_m1	1.66 ↑	1.88 ↑
IKBKE	Hs01063858_m1	2.57 ↑[a]	2.85 ↑[a]
IKBKG	Hs00175318_m1	2.01 ↑	2.04 ↑
LRDD	Hs00388035_m1	2.30 ↑[a]	4.07 ↑[b]
LTA	Hs99999086_m1	ND	ND
LTB	Hs00242739_m1	NC	NC
MCL1	Hs00172036_m1	1.37 ↑	1.64 ↑
NALP1	Hs00248187_m1	NC	2.01 ↑
NFKB1	Hs00765730_m1	1.57 ↑[a]	1.58 ↑
NFKB2	Hs00174517_m1	1.28 ↑	2.12 ↑
NFKBIA	Hs00153283_m1	NC	NC
NFKBIB	Hs00182115_m1	NC	NC
NFKBIE	Hs00234431_m1	1.86 ↑	1.87 ↑
NFKBIZ	Hs00230071_m1	NC	NC
PEA15	Hs00269428_m1	1.60 ↑	1.80 ↑
PMAIP1	Hs00560402_m1	1.25 ↑	1.81 ↑[a]
PYCARD	Hs00203118_m1	2.63 ↑[a]	3.25 ↑[a]
RELA	Hs00153294_m1	1.86 ↑	2.16 ↑
RELB	Hs00232399_m1	NC	NC
REL	Hs00968436_m1	1.23 ↑	1.52 ↑
RIPK1	Hs00169407_m1	2.08 ↑[a]	2.54 ↑[a]
RIPK2	Hs01572688_m1	1.59 ↓[b]	1.43 ↓[a]
TA-NFKBH	Hs01076336_m1	2.13 ↑[a]	2.44 ↑[a]
TBK1	Hs00179410_m1	1.32 ↑	1.72 ↑
TNF	Hs00174128_m1	2.28 ↓[a]	2.96 ↓[a]
TNFRSF10A	Hs00269492_m1	1.57 ↑	2.20 ↑[a]
TNFRSF10B	Hs00366272_m1	1.80 ↑[a]	2.34 ↑[a]
TNFRSF1A	Hs01042313_m1	NC	NC
TNFRSF1B	Hs00153550_m1	2.42 ↑[a]	2.80 ↑[b]
TNFRSF21	Hs00205419_m1	1.57 ↑	1.89 ↑[a]
TNFRSF25	Hs00980365_g1	1.66 ↑	1.66 ↑
TNFSF10	Hs00234356_m1	2.93 ↑[a]	3.66 ↑[a]
TRADD	Hs00601065_g1	1.77 ↑	2.29 ↑[a]

Numbers represent the fold change for specified genes. NC stands for no change. ND stands for not determined. ↑ indicates an up-regulation. ↓ indicates a down-regulation. A P-value ≤0.05 ([a]) or ≤0.01 ([b]) indicates a significant change relative to treatment with PTX alone.

(Figs. 3 and 4). In MDA-MB-231 cells, combination treatment resulted in a non-statistical increase in intracellular PTX. On the contrary, when HL-60 cells were treated with PTX alone or in combination with 2.5 ng/ml CPT, intracellular PTX was not detected by HPLC.

Expression of apoptosis-related genes upon exposure to PTX alone or in combination with CPT. To further explore the mechanism by which CPT obstructed PTX-induced apoptosis, we used a quantitative real-time PCR gene array analysis to determine the expression levels of several apoptosis-related transcripts. The TaqMan Low Density Array Human Apoptosis Panel consisted of assays for 93 human genes from multiple pathways involved in apoptosis. In addition to the 93 target genes the array contained three endogenous controls (18S, ACTB, GAPDH). In PANC-1 cells treated with a combination of 100 ng/ml PTX and 2 ng/ml CPT or 100 ng/ml PTX and 4 ng/ml CPT, as compared to those treated with PTX alone, 36 genes were found to be up-regulated with fold change of 2 or higher (Table I). Of those 36 genes, 29 genes showed statistically significant differences from PTX alone treatment according to a two sample equal variance, one-tailed t-test. Additionally, 2 genes were significantly down-regulated with fold changes of 2 or higher. Interestingly, four anti-apoptotic genes (*BCL2L10*, *CFLAR*, *HIP1* and *TRADD*) were up-regulated by PTX and CPT combination treatment.

Discussion

The cellular processes controlling synergy or antagonism between cancer therapeutic agents used in combination are currently the subject of intense investigation (2,22-25). As many cancers do not fully respond to single-agent treatment, the development of a combination therapy utilizing two common and potent chemotherapeutics such as PTX and a topo I inhibitor holds enormous potential for the treatment of several malignancies. However, the number of studies which evaluate the specific combination of PTX and topo I inhibitors against tumor growth is limited. Furthermore, in previous *in vitro* studies, this combination has been found to be synergistic (17,19), antagonistic (18) or both (19) depending on the tumor samples studied. Our present study was conducted to shed additional light on the interaction between PTX and CPT by testing the effect of combination treatment on cell viability, apoptosis and cellular pharmacokinetics of PTX. The human tumor cell lines examined in this study were of different histological origin and included a pancreatic carcinoma (PANC-1), a breast carcinoma (MDA-MB-231), and a leukemia (HL-60) to have a more comprehensive analysis on cellular response patterns to combination drug treatment.

The current studies were performed using rubusoside-solubilized PTX and CPT, which allowed examination of the drug combination without the use of DMSO or other co-solvents. This is the first report on this novel approach to solubilizing PTX and CPT. It is noteworthy that CPT in its original structure, not as a modified analogue (topotecan or irinotecan), was also examined for the first time without the use of organic solvents. In many *in vitro* assays, including cell viability and apoptosis assays, the upper limit of organic solvents (e.g., DMSO, ethanol) is often kept to a maximum 1% v/v to minimize or avoid solvent effects on the physiology of the cells. When comparing the effects of the commonly used DMSO co-solvent approach and a novel rubusoside approach for solubilizing PTX, it was unexpected to find that DMSO-solubilized PTX was no longer detectable by HPLC when diluted to 1% aqueous DMSO. This result indicated that, in an aqueous DMSO solution, PTX was in a suspension, whereas in the aqueous rubusoside solution PTX was completely solubilized. Centrifugation or filtration tends to remove PTX from a suspension but not from a solution. This finding raises questions on the accuracy and reliability of the 1% DMSO co-solvent approach to solubilizing water-insoluble compounds and serves as a precaution to drug discovery efforts that may possibly underestimate the biological effects of otherwise potent compounds. This finding also clearly points to the importance of using an established method to analyze solubilized samples rather than relying on assumed dilution concentrations, if drug activity data are to be correctly interpreted. Finally, this finding prevented the inclusion of soluble DMSO drug controls for these experiments. Therefore, rubusoside was used for all subsequent experiments regarding the interaction between PTX and CPT. Cell viability and apoptosis assays on cells incubated with rubusoside alone confirmed the non-toxic nature of this compound (Figs. 2-4). Although this is the first report on the novel approach for solubilizing PTX and CPT with rubusoside, a complete study of rubusoside cytotoxicity is beyond the scope of this study and will be the subject of future investigations.

Our findings demonstrated the interaction between PTX, a microtubule stabilizing agent, and CPT, a topo I inhibitor, to be antagonistic in PANC-1 and MDA-MB-231 cells, but not in HL-60 cells (Figs. 2-4). This finding supports a previous report demonstrating that interactions between PTX and CPT vary and are dependent on cellular context (19). To investigate the mechanism by which CPT antagonized the cytotoxic and apoptotic effects of PTX, the intracellular accumulation of PTX was quantified. It was suspected that the use of CPT could block the cellular accumulation of PTX, thereby enabling the cell to avoid cytotoxic drug exposure. However, PTX not only accumulated in the cells to the same concentration when used alone, but increased when CPT was introduced to the cell culture (Fig. 5). This finding is important because it excludes the possibility that CPT is blocking the intracellular accumulation of PTX and points to other possible mechanisms of antagonism. One of which is genetic mutation leading to altered tubulin structure and decreased binding by PTX (26). This phenomenon would result in reduced efficacy of PTX in cells and provides a strong rationale to investigate the intracellular changes that decouple PTX from its targets. In contrast, when HL-60 cells were treated with PTX alone or in combination with CPT, intracellular PTX was not detected by HPLC. This was probably due to the high amount of cytotoxicity at the drug concentrations tested, resulting in low recovery of HL-60 cellular material. Therefore, the amount of intracellular PTX may have been below the limit of detection by HPLC.

Another possible mechanism behind the observed antagonism in PANC-1 and MDA-MB-231 cells is that the apoptotic pathway induced by CPT is dominant and allows the cell to

circumvent the apoptotic program induced by PTX. Therefore, a TaqMan Low Density Array Human Apoptosis Panel was used to evaluate any changes in apoptosis at the level of gene expression upon treatment with PTX alone or in combination with CPT. Our data revealed that several genes were up-regulated upon exposure to PTX, and co-incubation with CPT altered the expression of these transcripts in a dose-dependent manner (Table I). Interestingly, a comparison of gene expression in PANC-1 cells showed that a small number of anti-apoptotic genes (*BCL2L10*, *CFLAR*, *HIP1* and *TRADD*) were up-regulated upon combination treatment with PTX and CPT, as compared to treatment with PTX alone. As apoptosis signaling involves many players and is a complex balance between strictly controlled inputs of pro- and anti-apoptotic signals, the specific roles that these genes play in mediating the antagonistic effect of CPT against PTX-induced apoptosis is not known and will be the subject of future investigations.

In summary, rubusoside-solubilized PTX and CPT each maintained cytotoxic activity against all three human cancer cell lines tested. However, the combination of PTX and CPT was antagonistic in PANC-1 and MDA-MB-231 cell lines and non-interactive in HL-60 cells. The observed antagonism between PTX and CPT was not due to a reduced intracellular accumulation of PTX, suggesting that other mechanisms are involved. Our data indicate that the combination altered the expression of genes involved in apoptosis as compared to treatment with PTX alone, but the exact roles of these genes remain unknown. Future investigations will be required to fully elucidate the mechanistic interactions between PTX and CPT. However, it is apparent that the assumed synergy between these two mechanistically different chemotherapeutic agents was not supported by the results of this study. Therefore, precautions must be taken when designing combinational therapies where a suggested synergistic benefit may not exist.

Acknowledgements

We would like to thank Karen McDonough in the LSU Agricultural Center Cell Culture Core for providing all cell lines and for technical assistance with cell culture. We also thank Rhett Stout for critical review of the manuscript. This research was supported in part by the BAIT Program, LAES Technology Transfer Fund of the LSU Agricultural Center, and the McIntire-Stennis Fund.

References

1. Mekhail TM and Markman M: Paclitaxel in cancer therapy. Expert Opin Pharmacother 3: 755-766, 2002.
2. Oliveras-Ferraros C, Vazquez-Martin A, Colomer R, De Llorens R, Brunet J and Menendez JA: Sequence-dependent synergism and antagonism between paclitaxel and gemcitabine in breast cancer cells: the importance of scheduling. Int J Oncol 32: 113-120, 2008.
3. Blagosklonny MV and Fojo T: Molecular effects of paclitaxel: myths and reality (a critical review). Int J Cancer 83: 151-156, 1999.
4. Wang TH, Wang HS and Soong YK: Paclitaxel-induced cell death: where the cell cycle and apoptosis come together. Cancer 88: 2619-2628, 2000.
5. Marupudi NI, Han JE, Li KW, Renard VM, Tyler BM and Brem H: Paclitaxel: a review of adverse toxicities and novel delivery strategies. Expert Opin Drug Saf 6: 609-621, 2007.
6. Slamon DJ, Leyland-Jones B, Shak S, *et al*: Use of chemotherapy plus a monoclonal antibody against HER2 for metastatic breast cancer that overexpresses HER2. N Engl J Med 344: 783-792, 2001.
7. Haddad R, Sonis S, Posner M, *et al*: Randomized phase 2 study of concomitant chemoradiotherapy using weekly carboplatin/paclitaxel with or without daily subcutaneous amifostine in patients with locally advanced head and neck cancer. Cancer 115: 4514-4523, 2009.
8. Stathopoulos GP, Dimitroulis J, Antoniou D, *et al*: Front-line paclitaxel and irinotecan combination chemotherapy in advanced non-small cell lung cancer: a phase I-II trial. Br J Cancer 93: 1106-1111, 2005.
9. Thomas CJ, Rahier NJ and Hecht SM: Camptothecin: current perspectives. Bioorg Med Chem 12: 1585-1604, 2004.
10. Basili S and Moro S: Novel camptothecin derivatives as topoisomerase I inhibitors. Expert Opin Ther Pat 19: 555-574, 2009.
11. Kingsbury WD, Boehm JC, Jakas DR, *et al*: Synthesis of water-soluble (aminoalkyl) camptothecin analogues: inhibition of topoisomerase I and antitumor activity. J Med Chem 34: 98-107, 1991.
12. Sawada S, Okajima S, Aiyama R, *et al*: Synthesis and antitumor activity of 20(S)-camptothecin derivatives: carbamate-linked, water-soluble derivatives of 7-ethyl-10-hydroxycamptothecin. Chem Pharm Bull (Tokyo) 39: 1446-1450, 1991.
13. Hsiang YH, Hertzberg R, Hecht S and Liu LF: Camptothecin induces protein-linked DNA breaks via mammalian DNA topoisomerase I. J Biol Chem 260: 14873-14878, 1985.
14. Lorence A and Nessler CL: Camptothecin, over four decades of surprising findings. Phytochemistry 65: 2735-2749, 2004.
15. Ramalingam SS, Foster J, Gooding W, Evans T, Sulecki M and Belani CP: Phase 2 study of irinotecan and paclitaxel in patients with recurrent or refractory small cell lung cancer. Cancer 116: 1344-1349, 2010.
16. Younes A, Preti HA, Hagemeister FB, *et al*: Paclitaxel plus topotecan treatment for patients with relapsed or refractory aggressive non-Hodgkin's lymphoma. Ann Oncol 12: 923-927, 2001.
17. Chou TC, Motzer RJ, Tong Y and Bosl GJ: Computerized quantitation of synergism and antagonism of taxol, topotecan, and cisplatin against human teratocarcinoma cell growth: a rational approach to clinical protocol design. J Natl Cancer Inst 86: 1517-1524, 1994.
18. Kaufmann SH, Peereboom D, Buckwalter CA, *et al*: Cytotoxic effects of topotecan combined with various anticancer agents in human cancer cell lines. J Natl Cancer Inst 88: 734-741, 1996.
19. Jonsson E, Fridborg H, Nygren P and Larsson R: Synergistic interactions of combinations of topotecan with standard drugs in primary cultures of human tumor cells from patients. Eur J Clin Pharmacol 54: 509-514, 1998.
20. Trubetskoy O, Marks B, Zielinski T, Yueh MF and Raucy J: A simultaneous assessment of CYP3A4 metabolism and induction in the DPX-2 cell line. AAPS J 7: E6-E13, 2005.
21. Hoffmann J, Vitale I, Buchmann B, *et al*: Improved cellular pharmacokinetics and pharmacodynamics underlie the wide anticancer activity of sagopilone. Cancer Res 68: 5301-5308, 2008.
22. Judson PL, Watson JM, Gehrig PA, Fowler WC Jr and Haskill JS: Cisplatin inhibits paclitaxel-induced apoptosis in cisplatin-resistant ovarian cancer cell lines: possible explanation for failure of combination therapy. Cancer Res 59: 2425-2432, 1999.
23. Reinicke KE, Kuffel MJ, Goetz MP and Ames MM: Synergistic interactions between aminoflavone, paclitaxel and camptothecin in human breast cancer cells. Cancer Chemother Pharmacol 66: 575-583, 2009.
24. Kang HJ, Lee SH, Price JE and Kim LS: Curcumin suppresses the paclitaxel-induced nuclear factor-kappaB in breast cancer cells and potentiates the growth inhibitory effect of paclitaxel in a breast cancer nude mice model. Breast J 15: 223-229, 2009.
25. Bruzzese F, Rocco M, Castelli S, Di Gennaro E, Desideri A and Budillon A: Synergistic antitumor effect between vorinostat and topotecan in small cell lung cancer cells is mediated by generation of reactive oxygen species and DNA damage-induced apoptosis. Mol Cancer Ther 8: 3075-3087, 2009.
26. Kavallaris M: Microtubules and resistance to tubulin-binding agents. Nat Rev Cancer 10: 194-204, 2010.